SOILS, SEC 5 · SOIL AND LANDSCAPE ECOLOGY · RESEARCH ARTICLE

Contamination characteristics, source analysis, and spatial prediction of soil heavy metal concentrations on the Qinghai-Tibet Plateau

Haolin Du[1] · Jinsong Wang[1,2] · Ying Wang[1] · Yubi Yao[1] · Xiaoyun Liu[1] · Yue Zhou[3]

Abstract

Purpose Soil heavy metal distribution is a key issue in environmental and health research. In recent years, an increasing number of anthropogenic disturbances have been identified on the Qinghai-Tibetan Plateau, leading to increased heavy metal contamination of soils. Therefore, this study investigated the distribution, sources, ecological risk, and prediction of heavy metals in soils on the Qinghai-Tibetan Plateau.

Material and methods Here, for each of the seven heavy metals (i.e., Cr, Ni, Cu, Zn, As, Cd, and Pb) investigated in the soil of the Qinghai-Tibet Plateau, we collected soil concentration values from the literature and carried out field sampling to generate new data. We then assessed the pollution characteristics and sources of soil heavy metals on the Qinghai-Tibet Plateau using geostatistics, positive matrix factorization model (PMF), disjunctive kriging, and mapped the pollution risk probability distribution of each heavy metal element.

Results and discussion Spatial autocorrelation was found for all seven heavy metals in the soils. Under different land-use types, the average concentrations of Cr, As, and Cd were highest in the water areas; Ni levels were highest in woodland; and Cu, Zn, and Pb concentrations were highest in residential, industrial, and mining lands. Using analysis by the PMF model and correlation analysis, four heavy metal sources were identified, including industrial sources and atmospheric deposition (Cd), traffic emissions (Cr, Zn, and Zn), natural sources (Ni and As), and mining activities (Cr and Pb). The pollution risk probabilities of Cr, Ni, Cu, Zn, As, and Pb were low in most areas of the Qinghai-Tibet Plateau, whereas the pollution risk probability of Cd was high over 29% of the area of the Qinghai-Tibet Plateau.

Conclusion The results highlighted no potential contamination for Cr, local potential contamination for Ni, Cu, Zn, As and Pb, while Cd exhibits more extensive contamination in the soils of the Qinghai-Tibet Plateau. Cd reduction should therefore be considered an important component of the strategy, policy, and action plan for soil pollution management on the Qinghai-Tibet Plateau.

Keywords Qinghai-Tibet Plateau · Soil · Heavy metals · Geostatistical analysis · Sources · Disjunctive kriging

---

✉ Jinsong Wang
  wjsgsmb_cn@sina.com

1 Key Laboratory of Arid Climatic Change and Reducing
   Disaster of Gansu Province, Key Open Laboratory of Arid
   Climate Change and Disaster Reduction of CMA, Institute
   of Arid Meteorology, CMA, Lanzhou 730020, China

2 Gansu Key Laboratory of Arid Climatic Change
   and Reducing Disaster, Key Laboratory of Arid Climatic
   Change and Disaster Reduction, Lanzhou Institute of Arid
   Meteorology of China Meteorology Administration,
   Lanzhou 730020, China

3 Hubei Key Laboratory for Heavy Rain Monitoring
   and Warning Research, Institute of Heavy Rain, CMA,
   Wuhan 430205, China

1 Introduction

Environmental heavy metal (HM) pollution has become a serious problem worldwide, especially in China, where soil pollution is particularly serious. The 2014 National Soil Pollution Survey Bulletin shows that the total exceedance rate of soil pollution in China reached 16.1%, with inorganic pollutants dominating, accounting for about 80% of the total pollution. HMs, among the most important inorganic pollutants, are difficult to eliminate from soil or water, are persistent, and bioaccumulative, and pose a great threat to food safety and human health (Huang et al. 2018). HMs have now become a hotspot of concern for the general public and a primary problem that needs to be addressed urgently.

Therefore, it is particularly important to identify the spatial variability of HMs in soils and to identify their sources and the environmental risks they represent.

In recent years, researchers in China and abroad have conducted many studies on the spatial correlation and variability of soil HMs (Chandra et al. 2014; Wu et al. 2017; Yoon et al. 2022), mainly using a coefficient of variation, semivariance function theory, and analysis of scale variance methods to analyze the spatial correlation, spatial structure, variation pattern, and sources of soil HMs in the study areas. Recently, geostatistical methods have become more widely used in the study of the spatial distribution and risk assessment of HMs (Lee et al. 2020). Ordinary kriging is able to achieve the best, unbiased estimation for unsampled areas and is the most commonly used method in spatial prediction. However, in practical applications of pollution assessment and risk management, the researcher may not be concerned with the HM concentration at a given location in space, but with the probability distribution of the risk above or below a certain threshold. The disjunctive kriging method can determine the risk probability of a single variable within a certain threshold (Goovaerts et al. 1997; Juang and Lee 2000) so that the environmental risk assessment of HMs estimated in this way has good application prospects.

In order to avoid the threats caused by HMs, it is important to identify potential sources of contamination (Jin et al. 2019). Available studies suggest that the spatial distribution of HMs in soils may be attributable to geological or anthropogenic sources (Hou et al. 2017). The distribution of naturally occurring HMs may be highly heterogeneous, with some land-use types showing significantly elevated HM concentrations. Human activities, including mining, manufacturing, agriculture, urban runoff, and atmospheric deposition, result in significantly elevated HM concentrations in localized areas. To effectively control the health risks caused by HMs in soils, it is necessary to identify and quantify potential sources of contamination, especially those caused by human activities (Romic and Romic 2003). The positive definite matrix factor analysis model (PMF), recommended by the United States Environmental Protection Agency is widely used because its factor matrix is constrained to be non-negative, allowing more meaningful factors to be obtained (Tian et al. 2018). This model was first applied to the source analysis of the atmospheric particulate matter, but in recent years its use has been extended to the traceability studies of HMs in water, soil, and sediment, and the results have shown that the model can clearly identify the pollution sources and assign their contribution to each HM (Zhang et al. 2018; Chen et al. 2016).

The Qinghai-Tibet Plateau or Tibetan Plateau, known as the "third pole" of the Earth, is the region where the "air–water-ice-biospher" multi-layers are most fully reflected and where they interact most strongly, and its ecological function is an important barrier to ensure ecological security in China and Asia (Wu et al. 2018; Guo et al. 2018). Under the continuous influence of human activities, the land use of the Qinghai-Tibet Plateau has changed dramatically recently, and the changes in the degree of fragmentation and aggregation, and the complexity of the landscape shape will further damage vegetation, water supply, and soil, leading to direct or indirect contamination of soil with HMs and increasing the possibility of redistribution and migration of these elements in the soil (Wu et al. 2016). HMs have been reported to have been detected in biota on the Qinghai-Tibet plateau, with relatively high levels of Cu and Zn, reaching maximum concentrations of 2.0 and 6.9 µg/g, respectively (Yang et al. 2007). HMs were also widely present in different environmental matrices, with maximum concentrations of Cr and As reaching 155.54 and 19.27 mg/kg in Tibetan soils. water samples from the Salween River contained high levels of Pb and Ni, with maximum values of 781 and 18 µg/L, respectively; and water samples from the Yarlung Tsangpo River contained high levels of Pb, Zn, and Ni, with maximum values of 130, 29, and 104 µg/L, respectively (Sheng et al. 2012; Huang et al. 2008). This shows that HM pollution of the Qinghai-Tibet Plateau cannot be ignored. However, current studies have mainly focused on studying the distribution of HMs in the environment of the Qinghai-Tibet Plateau, evaluating the environmental health risks caused by HMs; these results are highly diverse and fragmented, without providing sufficient information on the source identification of HMs in the soil of the Qinghai-Tibet Plateau, and prevent us from better understanding the current ecological situation in the Qinghai-Tibet Plateau.

Based on the above background, this paper takes the HMs in the soil of the Qinghai-Tibet Plateau as the research object, combines the semivariance function theory and geostatistical methods together, gives full play to the functionality of different methods, comprehensively analyzes the spatial correlations and the variability patterns of seven HMs in the soil of the Qinghai-Tibet Plateau, namely Cr, Cd, Cu, Pb, Zn, Ni, and As, and uses the PMF model to identify and quantify the potential HM pollution sources. The results may provide comprehensive information for an understanding of the distribution characteristics and sources of HMs in the soil of the Qinghai-Tibet Plateau and a basis for soil pollution prevention and control strategies in such high-altitude areas.

2 Materials and methods

2.1 Overview of the study area

The Qinghai-Tibet Plateau is located in the west of China (26°00'–39°47'N, 73°19'–104°47'E) and is the largest

plateau in China and the highest in the world (Fig. 1). The main vegetation landscape is alpine and alpine land, and the main climate type is plateau mountain climate with strong sunshine, and significant seasonal differences in dryness and humidity, with cool and rainy summers, and long, dry, and cold winters. The geology of the Qinghai-Tibet Plateau is complex, consisting mainly of clastic sedimentary and metamorphic rocks in the south, and volcanic rocks, clastic sandstones, shales, and marls in the north-central part (Li 2010). With high to low altitudes, zonal soils such as cold desert soils, meadow soils, steppe soils, and yellow–brown soils are widely distributed on the Qinghai-Tibet plateau, with generally low development and predominantly physical weathering.

2.2 Sample collection and analysis

During the study period 2020–2022, we conducted field sampling in eastern Qinghai Province, central Tibet, and Gannan Tibetan Autonomous Prefecture. The actual geographic coordinates of the sampling sites were obtained using a handheld global positioning system (GPS), and each sample consisted of five subsamples, with > 1 kg of soil guaranteed at each location. During the sampling period, the ground at the sampling sites was dry, or the ground was dry for at least 7 days after rainfall. 42 topsoil samples were collected in the east of Qinghai Province, 34 topsoil samples were collected in central Tibet, and 50 topsoil samples were collected in Gannan Tibetan Autonomous Prefecture. The soil samples were naturally dried to remove debris such as plant residues and gravels, and the soil was ground and sieved through a 200-mesh sieve according to the quadrat method [25]. The soil samples were extracted with aqua regia and digested with an inductively coupled digestion instrument (Multiwave PRO) to a volume of 25 mL [26].

The samples were measured in parallel double samples at 10% and the relative deviation should be less than 30%; the samples were analysed with 10% spiked recovery samples and the spiked recovery should be controlled between 70 and 125%.

At the same time, we searched Google Scholars and Science Net with the keyword "heavy metal," "soil," "heavy metals," and "Qinghai Tibet Plateau", and selected more than 70 related papers. After sorting out the literature, we found that the geographic location of soil sampling in most of the literature was not clearly described (that is, there was no latitude and/or longitude). Finally, the data of Cu, Zn, and Pb in 168 topsoil (0-20 cm), Cr, Ni, and Cd in 166 topsoil (0-20 cm), and As in 163 topsoil (0-20 cm) were collected (Table S1).

2.3 Analysis of semi-variance functions

The semivariance geostatistical function model is a geostatistical analysis method and is the most commonly used metric to characterize the spatial variability of regionalized variables and was used to understand the multi-scale spatial variability of soil HMs on the Qinghai-Tibet Plateau. The nugget parameter (C_0) represents the random spatial variance of soil HMs. The partial abutment parameter (C) indicates the structural spatial variance of soil HMs. A high bias abutment value implies that a large portion of the spatial variation is due to regional-scale influences. The sill parameter ($C_0 + C$) represents the total degree of spatial variability of soil HMs. The spatial variability can be classified according to the ratio of the nugget parameter to the sill parameter (nugget gold coefficient). The nugget gold effect indicates the proportion of spatial variability caused by the random component to the overall variability. A nugget gold coefficient of less than 25% indicates a strong spatial correlation of soil HM elements; 25 to 50% indicates a significant
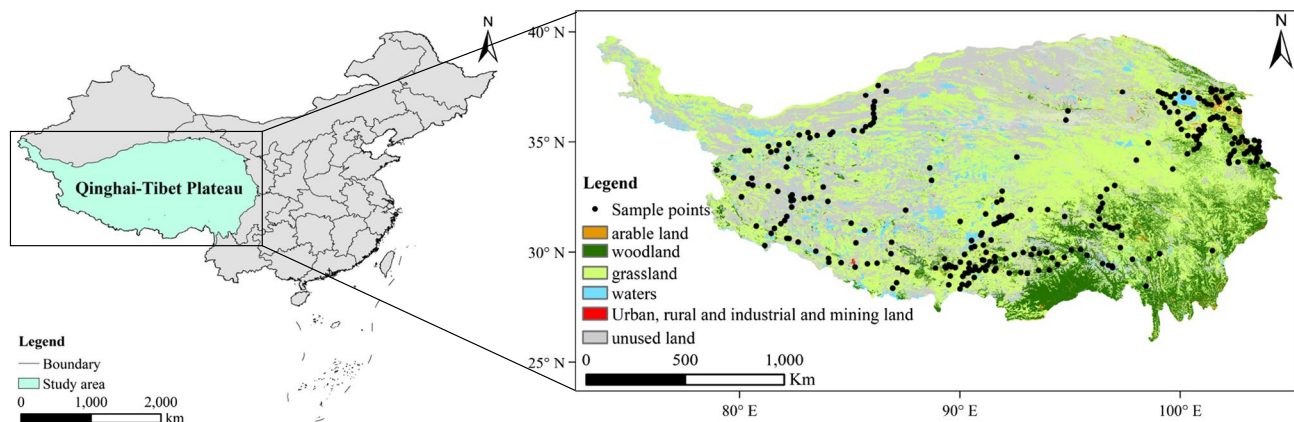

Fig. 1 Study area and sampling sites

spatial correlation of soil HM elements; 50 to 75% indicates a moderate spatial correlation of soil HM elements; greater than 75% indicates a weak spatial correlation of soil HM elements and the variability consists mainly of random variation (Burgos et al. 2006; Hu et al. 2018; Lin et al. 2018).

Since parametric statistical analysis requires data to be normally distributed, spatial analysis was preceded by the Shapiro–Wilk normality test. If $P_{s-w} > 0.05$, the data were considered to obey normal distribution; otherwise, data transformation was required. The semivariance function was calculated and fitted with GS + 9.0 software (https://geostatistics.com/).

2.4 Spatial autocorrelation analysis

Spatial autocorrelation analysis refers to the degree of correlation between the values of the same attribute of a variable on neighbouring spatial units and includes both global and local spatial autocorrelation analysis. Global spatial autocorrelation analysis uses Moran's I index to reflect the spatial aggregation of soil HMs over the entire study area. Moran's I is calculated as:

$$I = \frac{n \sum_{i=1}^{n} \sum_{j=1}^{n} W_{ij}(x_i - \bar{x})(x_j - \bar{x})}{\sum_{i=1}^{n} \sum_{j=1}^{n} W_{ij} \sum_{i=1}^{n}(x_i - \bar{x})^2} \quad (1)$$

where I is the Moran index; n is the number of areas in the soil HM content space; x_i is the elemental HM content of the soil in the ith region; x_j is the elemental content of soil HMs in the jth area; $\bar{x}$ is the average of the soil HM content in the study area; W_{ij} is the spatial weight matrix, generally a symmetric array.

Local indicators of spatial association (LISA) reflect the extent to which soil HM in one sampling area is related to that in neighbouring sampling areas. Moran's I's LISA is calculated as:

$$I_i = \frac{x_i - \bar{x}}{s^2} \sum_{j=1}^{n} W_{ij}(x_j - \bar{x}) \quad (i \neq j) \quad (2)$$

where S is the standard deviation of x_i; I_i is the local spatial autocorrelation index.

The global spatial autocorrelation analysis is based on Moran's I, which reflects the spatial distribution of HMs in the sampling area on the Tibetan Plateau, and ranges from [- 1, 1]. If Moran's I is greater than 0, it means that there is a positive spatial correlation in the study area; if Moran's I is less than 0, it means that there is a negative spatial correlation in the study area; if Moran's I is equal to 0, it means that there is no autocorrelation in the study area and the distribution is random. If Moran's I is equal to 0, the study area is not autocorrelated and is randomly distributed.

2.5 Source resolution model

The basic principle of PMF source resolution is as follows (Guan et al. 2018). Assume that the matrix X is the measured sample data, the matrix X can be broken down into a fraction matrix G and a load matrix F, and the residual matrix E represents the difference between the matrix X_{ij} and the model matrix Y_{ij}. The basic equation is as follows:

$$E_{ij} = X_{ij} - Y_{ij} = X_{ij} - \sum_{h=1}^{p} G_{ih}F_{hj}(i = 1, \cdots, m; j = 1, \cdots n) \quad (3)$$

where E_{ij} is the residual matrix; G_{ih} is the contribution of sample i in the hth source, which is the source fraction matrix, and F_{hj} is the concentration of pollutant j in source h, which is the source loading matrix.

The PMF model divides the experimental measured data into two matrices of contribution with coefficients (G) and number of factors (F), and, using the pollutant concentration and uncertainty of each sampling point, the measured data are weighted according to the weighting factor for each point to obtain the minimum objective function Q:

$$Q = \sum_{i=1}^{n} \sum_{j=1}^{m} \left[\frac{X_{ij} - \sum_{k=1}^{p} G_{ik}F_{kj}}{u_{ij}} \right] \quad (4)$$

where Q is the cumulative residual, i is the number of samples, and j is the type of contaminant measured; p is the number of suitable factors found by the PMF model; F is the composition matrix for each source; G is the contribution matrix for each contaminant in the sample; and u_{ij} is the uncertainty for each sample/contaminant type, calculated as follows:

$$u_{ij} = \begin{cases} \frac{5}{6} \times L_{MDL} \left(x_{ij} \leq L_{MDL} \right) \\ \sqrt{\left(RSD \times x_{ij}\right)^2 + \left(L_{MDL}\right)^2} \end{cases} \quad (5)$$

where RSD is the relative standard deviation of HMs concentration, L_{MDL} is the method detection limit, and x_{ij} is the HMs sample concentration.

The signal-to-noise (S/N) ratio, which is the main diagnostic technique of the model, is able to indicate whether the variability in the measured values is real or a disturbance in the data. The smaller the S/N ratio, the more unstable this chemical element is in the model, and the less likely the sample will be detected. The factor number of the PMF modle is determined by the analytical results of several trials, errors, and relative changes in Q values (Reff et al. 2007).

2.6 Land cumulative index method

The ground accumulation index method takes into account the influence of natural diagenesis on the background values

and also the influence of anthropogenic activities on the environment (Müller 1969). It is calculated by the following equation:

$$I_{geo} = \log_2\left[C_i/\left(K \times C_n^i\right)\right] \qquad (6)$$

where I_{geo} is the ground cumulative index of HMs, C_i is the measured concentration of HM i, and C_n^i is the reference background value of HM i. In this paper, the background value of the soil environment on the Qinghai-Tibet Plateau is adopted as the reference value (Sheng et al. 2012), and K is used to eliminate the difference in background value that may be caused by the difference of rocks everywhere (generally taken as 1.5). The pollution levels are divided into seven levels, as shown in Table 1.

2.7 Disjunctive kriging

Using the disjunctive kriging technique, it is possible to obtain a conditional probability map of the measured indicator variable being above a pre-determined tolerance level (threshold). It provides an estimate of the conditional probability that a random variable located at a point, or averaged over a block in two-dimensional space, exceeds certain thresholds. It is assumed that the concentration of a radionuclide is a realization of a random variable $Z(x)$, where x denotes the spatial coordinates in two dimensions. If a threshold concentration, z_c, is defined, marking the limit of what is acceptable, then the scale is dissected into two classes, which are less than and more than z_c, respectively. The soil must belong to one of these classes at any one place. The values 0 and 1, respectively, can be assigned to the two classes, thereby creating a new binary variable, or indicator, which is denoted by $Q[Z(x) \geq z_c]$ (Steiger et al. 1996; Lark and Ferguson 2004).

2.8 Data analysis

All statistical analyses were performed using SPSS 26.0 (IBM SPSS Inc., Chicago, USA) and Origin 2019 (Origin-Lab, Northampton, USA). PMF models were performed by EPA PMF v5.0 (USEPA, USA). Before performing the PMF models, the dataset was first examined to eliminate outliers based on histograms and quartiles, since outliers have a significant impact on the PMF models. The spatial autocorrelation of soil HM content was carried out using GeoDA

spatial analysis software and the results were imported into ArcGIS 10. 4 (Esri Inc., California, USA) software for correlation mapping. Kriging interpolation with ArcGIS10.4 was applied to determine the spatial distribution of HMs and to provide information about the potential sources of soil contamination.

3 Results and discussion

3.1 Spatial distribution characteristics of heavy metals

The statistical results of the combined literature and sampling data are shown in Table 2. The average concentrations of the seven HMs did not exceed the national soil environmental quality standards (Ministry of Ecology and Environment of the People's Republic of China 2018); the average concentrations of Ni, Cu, Zn, As, and Cd exceeded the soil environmental background values of the Qinghai-Tibet Plateau (Sheng et al. 2012), with Cd (2.38 times the background value) being the most significant. Compared with the Chinese soil background values (Wei et al. 1991), the mean concentrations of Ni, Cu, Zn, As, and Cd were higher, with As (2.19 times higher) and Cd (1.96 times higher) being significantly higher. Compared with the world soil background value (Bowen 1979), only the mean concentration of As exceeded the world soil background value, reaching 4.37 times the background concentration.

The magnitude of the coefficient of variation of HMs concentration in the topsoil of the Qinghai-Tibet Plateau was Cd > As > Pb > Ni > Cu > Zn > Cr, in which the coefficient of variation of Cr was the smallest and belonged to moderate variability (20–50%), whereas the coefficients of Ni, Cu, Zn, As, and Pb belonged to high variability (50–100%), and Cd belonged to extreme variability (> 100%), indicating that human activities may be the main factor causing the high spatial heterogeneity of the elements Ni, Cu, Zn, As, Cd, and Pb.

3.2 Summary of heavy metal concentration geostatistics

3.2.1 Soil heavy metal spatial structural analysis

The results of the semivariance function fitting (Table 3) showed that four elements, Cu, As, Cd and Pb, fitted the

Table 1 Classification of heavy metal pollution levels

Project	Pollution level						
	Non-polluted	Light pollution	Moderate pollution	Moderate–severe pollution	Severe pollution	Severe–extreme pollution	Extreme pollution
Parameter	≤ 0	$0 < I_{geo} \leq 1$	$1 < I_{geo} \leq 2$	$2 < I_{geo} < 3$	$3 \leq I_{geo} < 4$	$4 \leq I_{geo} < 5$	≥ 5

Table 2 Descriptive statistical characteristics of soil heavy metals on the Qinghai-Tibet Plateau (mg/kg)

Element	Range	Mean	Median	SD[a]	CV[b]/%	China Soil Environmental Quality Standards	Background value		
							Qinghai-Tibet Plateau	China	World
Cr	9.78 ~ 429.00	84.1	55.3	243.0	289.0	250	77.40	61	70
Ni	4.08 ~ 285.10	32.3	25.4	29.6	91.9	190	32.10	26.90	50
Cu	5.97 ~ 107.90	22.5	20.0	11.5	51.4	100	21.90	22.60	30
Zn	25.94 ~ 574.38	94.0	76.7	74.6	79.3	300	73.70	74.20	90
As	1.83 ~ 172.69	26.2	17.5	28.6	109.0	25	18.70	11.2	6
Cd	0.03 ~ 2.04	0.2	0.1	0.2	114.9	0.6	0.08	0.097	0.35
Pb	4.20 ~ 153.90	30.0	24.5	21.5	71.6	170	28.90	26	35

[a]standard deviation

[b]coefficient of variation

spherical model, whereas two elements, Ni and Zn, fitted the exponential model, while Cr fitted the Gaussian model. The residuals of the seven elements were all well below 0.1, and the coefficients of determination were all greater than 0.5, indicating that the accuracy of each theoretical model met the requirements and each model explained the spatial structure adequately.

The spatial autocorrelation of Ni and As was strong, indicating that their spatial distribution patterns were less affected by human activities and showed strong spatial correlation, while structural factors, such as parent material, topography, and soil type, were the main causes of the spatial variation of the two elements. The basal effect values of Cr and Cd were greater than 75%, which were dominated by random factors, indicating that the spatial variation of these two elements on the Qinghai-Tibet Plateau was mainly caused by random factors, such as natural and human activities.

The variation range indicates the magnitude of the range of spatial autocorrelation, and the variables have spatial autocorrelation values within the range of variation, and vice versa. The variation range of the seven elements on the Qinghai-Tibet Plateau is Ni > Zn > As > Pb > Cd > Cr > Cu in descending order, among which the variation range of Ni is large, indicating that Ni has strong spatial autocorrelation over a large spatial range, whereas Cu has the smallest variation range and only has autocorrelation over a relatively small spatial range, so that the influence of local sources on Cu may be larger.

3.2.2 Spatial autocorrelation analysis of heavy metal content in soils

The results of the global autocorrelation analysis of soil HM element content on the Qinghai-Tibet Plateau are shown in Table 4. The Moran's I for soil HM element content on the Qinghai-Tibet Plateau are all greater than 0. From a global perspective, the soil HM element content has a certain spatially positive correlation distribution, i.e. soils with high soil HM element content are surrounded by high soil HM element content, and soils with low soil HM element content are surrounded by low soil HM element content. It also indicates that there is a certain aggregation of soil HM elements in the study area, with high and low aggregation of soil HM elements, where high values mean that the value in the sampling area is greater than the mean and low values mean that the value in the sampling area is less than the mean.

Table 3 Fitting results of semivariance functions

Element	Model type	Nugget	Sill	Nugget gold coefficient	r^2	Residual SS	Range/m
Cr	Gaussian	5.3114	6.0220	0.882	0.711	0.018	26700
Ni	Exponential	0.0020	0.0107	0.186	0.742	0.000	856107
Cu	Spherical	0.0704	0.1248	0.564	0.905	0.000	24800
Zn	Exponential	0.0039	0.0086	0.454	0.907	0.000	70500
As	Spherical	0.0264	0.1226	0.215	0.543	0.000	35800
Cd	Spherical	0.0007	0.0009	0.769	0.885	0.000	32600
Pb	Spherical	2.5022	4.3141	0.580	0.943	0.000	34189

Table 4 Moran's *I* of soil heavy metal content and results of Monte Carlo hypothesis test

Element	Moran's *I*	Z	P
Cd	0.139	4.279	0.001
Cr	0.207	6.085	0.001
Cu	0.146	4.655	0.001
As	0.203	6.146	0.001
Zn	0.147	4.347	0.001
Ni	0.061	1.997	0.034
Pb	0.358	10.416	0.001

In order to verify whether Moran's *I* was significant, the Monte Carlo iterative method was used to test the hypothesis of Moran's *I*. The number of iterations was 999, and the results of the global autocorrelation of soil HM elements were obtained (Table 4): all Z-values were greater than 1. 96, and all P-values were less than 0. 05, indicating that the spatial autocorrelation of Moran's *I* was statistically significant.

The results of the local spatial autocorrelation analysis of the soil HM element content on the Qinghai-Tibet Plateau are shown in Fig. 2, which shows the different characteristics of the soil HM element content distribution. The five soil HM elements Cr, Ni, Cu, As, and Pb are low in content and low in surrounding content (low-low), mainly in the Huangshui basin and Gannan Tibetan Autonomous Prefecture. The five soil HM elements Cr, Cu, Zn, As, and Pb are high in and around (high–high), and these areas are mainly found in the Yarlung Tsangpo river basin. The low concentrations of soil HM elements surrounded by high concentrations (low–high) and high concentrations of soil HM elements surrounded by low concentrations (high-low), which are sporadically distributed around high-high or low-low areas respectively, indicate a potential contamination risk in areas where low-value anomalies occur near high-value concentrations or high-value anomalies occur near low-value concentrations. The other areas are not significantly autocorrelated.

3.2.3 Distribution characteristics of heavy metals under different land-use types

Figure 3 shows the basic distribution statistics of the seven HMs under different land-use types, which are represented by a split-edge violin plot. The land-use type database was revised based on the field survey sampling points and Google Earth images, and the land-use types were allocated into six categories, namely: (1) arable land, (2) woodland, (3) grassland, (4) water area (floodplain soil along a river), (5) urban, rural, and industrial and mining land, (6) unused land. The land-use types in the study area were mostly grassland and unused land, accounting for 48.85% and 32.87% of the total area of the Qinghai-Tibet Plateau, respectively,

whereas arable land, woodland, water area, and urban, rural, industrial, and mining land accounted for 0.91%, 12.19%, 5.71%, and 0.10%, respectively. Comparing the HM concentrations in the soil of different land-use types, the mean concentration of Cr in all six land-use types was lower than the background value of the Qinghai-Tibet Plateau soil, and those of Cr in woodland and water areas were higher than the world soil background values; the mean concentration of Ni in different land-use types is lower than the world soil background value (Fig. 3). Furthermore, the mean concentrations of Ni in arable land, forest land, water areas, and urban, rural, industrial and mining land were greater than the world soil background value. The mean concentrations of Cu and Zn in urban, rural, industrial, and mining land were much higher than those in other land-use types, which further proves that human activities may be the main factor causing the increase in Cu and Zn concentrations, probably influenced by agriculture, industry, and transportation. The mean concentration of As in all six land-use types exceeded the world soil background value, among which the mean As concentrations in grassland, water, urban, rural and industrial, and mining land, and unused land exceeded the soil background value of the Qinghai-Tibet Plateau. The mean concentration of Cd in all the land-use types was higher than the soil background value of the Qinghai-Tibet Plateau, with the concentration in water being the highest, whereas the mean concentration of Pb in urban, rural, industrial, and mining land was the highest, exceeding the soil background values in the soil of the Qinghai-Tibet Plateau and the world soil background value (Fig. 3).

3.3 Source analysis of heavy metals

To effectively assign natural and anthropogenic sources to individual HMs, Pearson's correlation analysis was used to initially determine the correlation between the concentrations of the seven HMs. Next, the PMF model was applied to assign and quantify the potential sources of HMs (Fig. 4). To validate the results of the source assignments, the factor contributions of the PMF model were correlated with the Pearson correlation coefficients of the HMs (Fig. 4). The PMF model is a matrix analysis method based on iterative least squares, which discriminates the homologous information of each HM variable based on the value of the component's loading contribution (Paatero 1997). The difference between Q_{Robust} and Q_{Ture} was minimized when the number of factors was four. The majority of residuals followed a normal distribution between -3 and 3. The (S/N) ratio of all seven HMs was defined as "strong", and the coefficients of determination r^2 between observed and predicted concentrations were determined and were greater than 0.5 for all HMs except Cr, As, and Zn. Significantly related.
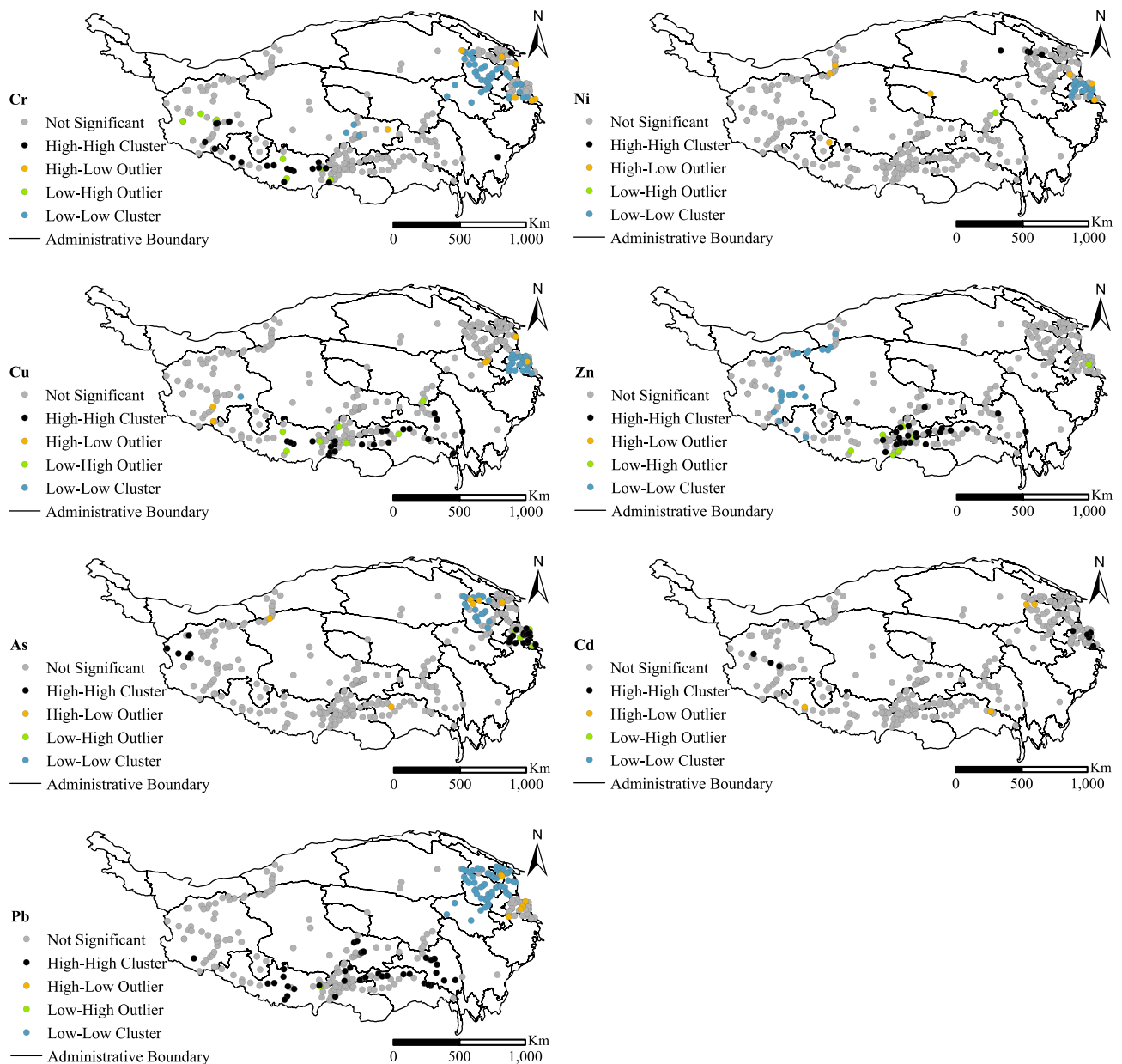
Fig. 2 Aggregation maps of local indicators of spatial association

A significant correlation ($r < 0.5$) was observed in Pearson's correlation coefficient matrix for HM concentration (Fig. 4c), which indicates a potential common source. Four factors (named Factors 1 to 4) were extracted from the PMF model, and their contribution percentages are shown in Fig. 4a. The PMF results indicate that the main loading element for Factor 1 was Cd and the main loading elements of Factor 2 were Cr, Cu, and Zn, whereas the main loading elements of Factor 3 were As and Ni and the main loading elements of Factor 4 were Cr and Pb (Fig. 4b).

The contribution of Factor 1 was 33.2% (Fig. 4), and the main characteristic element was Cd. Usually, atmospheric Cd deposition is an important source of soil Cd accumulation

(Liu et al. 2018), and waste gas (oil and coal combustion and municipal waste incineration) emissions are the main source of atmospheric Cd pollution, among which industrial waste gas emissions from developing regions such as West Asia and South Asia will increase the Cd enrichment on the Qinghai-Tibet Plateau through atmospheric transport (Dong et al. 2015). Emissions from the Tibetan plateau itself cannot be ignored, and pollutants produced during industrial production can also contaminate the soil directly or indirectly (Cheng 2003; Chen et al. 2017). Therefore, Cd contamination can be attributed to industrial sources and atmospheric deposition.

The contribution of factor 2 was 30.8% (Fig. 4), with the main characteristic elements being Cr, Cu, and Zn. The
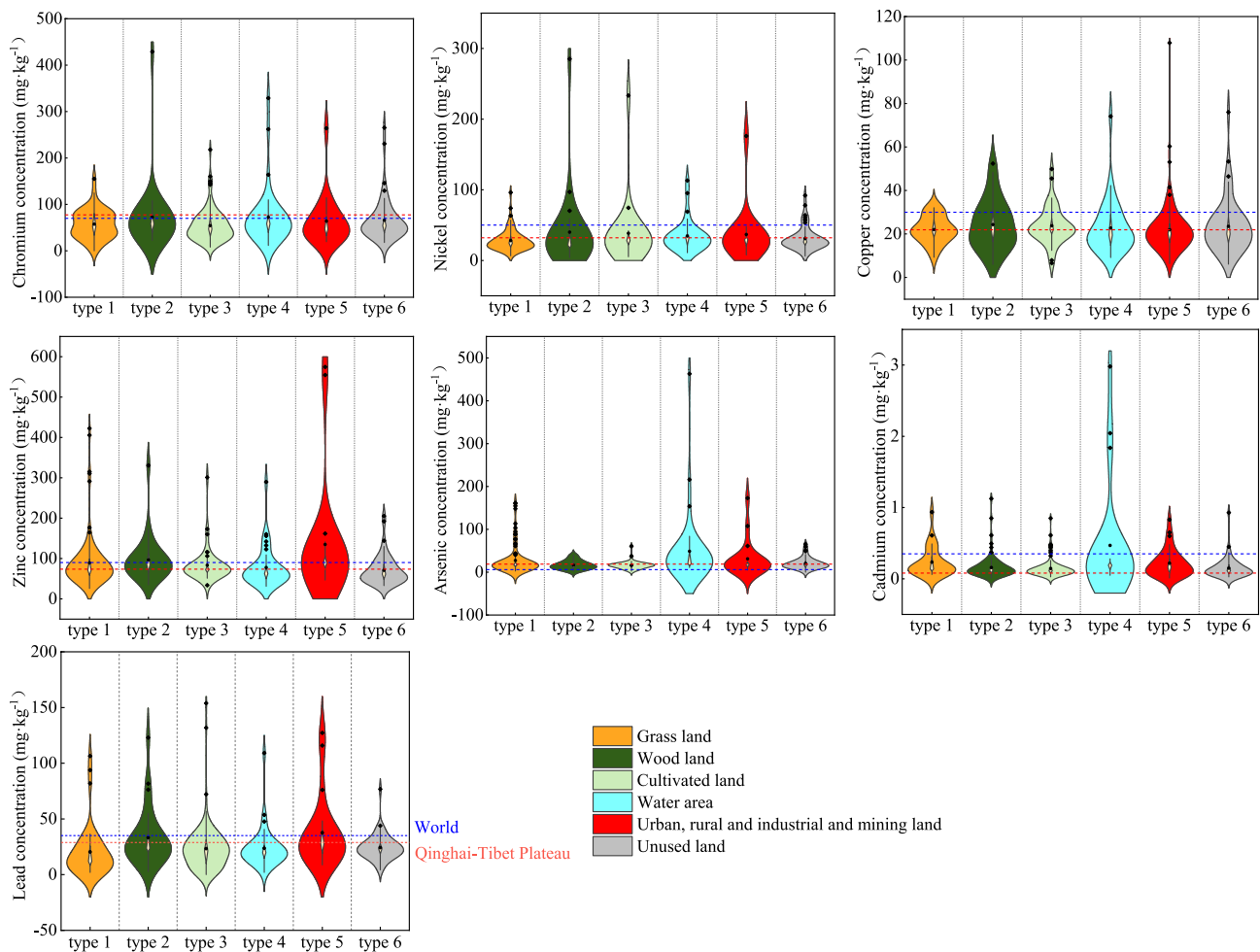
Fig. 3 Differences in heavy metal concentrations under different land-use types

results of Pearson correlation analysis showed a significant positive correlation between these three elements, indicating that they may have similar or identical sources. It is well known that Cr, Cu, and Zn are all important marker pollutants for motor vehicle emissions and brake pad wear, and are easily deposited and enriched in soil (Guan et al. 2017). The complexity of the current transportation network and regional connectivity in the Tibetan Plateau region is increasing (Zhao 2002), and the tourism economy is also putting greater pressure on the soil environment, with significant variability in soil trace elements along roadways. Therefore, Cr, Cu, and Zn can be categorised as traffic sources.

The contribution of Factor 3 was 2.6% (Fig. 4), and, in general, the two elements As and Ni are related to lithogenesis and soil parent material (Zhang et al. 2016); Pearson's correlation analysis showed a significant positive correlation between As and Ni concentrations, inferring that these two HMs have the same or similar sources. Some earlier studies have surfaced the geological formations of the Qinghai-Tibet Plateau and its evolutionary history, with dramatic changes in parent rocks in the

Kunlun, Qilian, and Himalayan mountain ranges, leading to a greater frequency and magnitude of changes in Ni and AS concentration levels and the phenomenon of background values of Ni and As in soils (Wu et al. 1992; Zhang et al. 2016). At the same time, geothermal activity has been shown to increase the enrichment of As in soils (Li et al. 2013). Therefore, As and Ni can be attributed to natural sources.

The contribution of Factor 4 was 33.4% (Fig. 4), and the main characteristic elements were Cr and Pb. The results of Pearson's correlation analysis showed a significant positive correlation between the two elements. The spatial distribution of Pb–Zn ores on the Qinghai-Tibet Plateau has a certain regularity and is concentrated in the Gangdis metallogenic belt and the Sanjiang metallogenic belt (Song et al. 2011). Among them, the Pb ore resources in the Gangdis metallogenic belt reach Gongbujiangda County in the east, Angren County in the west, and Zedang and Jiali Counties in the south and north. The Pb mineral resources of the Sanjiang metallogenic belt are located in the Hengduan Mountains area where the Nujiang, Lancang and Jinsha rivers flow together, spanning
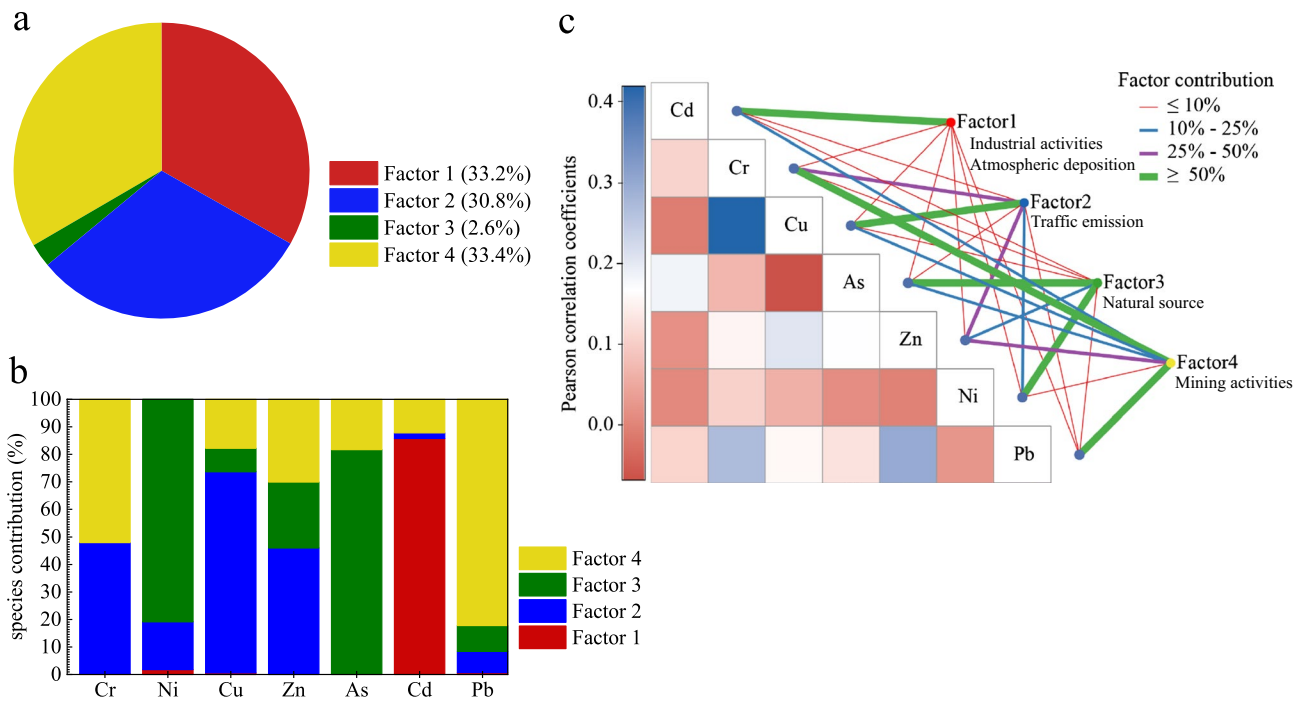
Fig. 4 Source apportionment of heavy metals in the study area. **a** The percentage of contribution for each factor by the PMF model. **b** Factor profiles of HMs in soils from the PMF model. **c** Identification of the correlations between HMs by combining Pearson's correlation coefficient analysis and the PMF model

eastern Tibet, western Sichuan, western Yunnan, and southern Qinghai (Cong et al. 2013; Gao et al. 2016), whereas the underground Pb concentration from industrial and mining purposes is the highest among the different land-use types. Chromite is one of the few types of minerals in severe shortage in China, and Tibet is the main source of chromite in China, with the Bangong Lake-Nujiang River suture zone starting from Bangong Lake in the west and turning southeast to extend out of Tibet along the Nujiang River valley through Changze and Dingqing, which is a remarkable zone with great potential for Cr–Ni mineralization. In recent years, with the implementation of the western development strategy of the central government and the opening of the Qinghai-Tibet Railway, as well as a large number of infrastructure construction projects, the regional metal mineral resources of the Qinghai-Tibet Plateau have been effectively developed, but at the same time, it has also brought serious damage to the ecological environment of the Qinghai-Tibet plateau, which can easily lead to soil erosion, HM pollution of water and soil, and pollution of the surface environment. Therefore, Cr and Pb sources can be classified as mining sources.

3.4 Spatial distribution characteristics of heavy metal contamination probabilities

The probability of contamination by the seven elements, Cr, Ni, Cu, Zn, As, Cd, and Pb, in the soil of the Qinghai-Tibet Plateau, was analyzed separately by using the disjunctive kriging method, and the distribution maps of the risk probability of contamination of soil by individual HMs were generated. The evaluation results of the accumulation index of Cr, Ni, Cu, Zn, As and Pb under the six types of land use types is less than 0; a slight pollution by Cd is present in grassland, woodland, waters and urban, rural and industrial and mining land, among which the accumulation index is highest in Urban, rural and industrial and mining land (Table 5). The seven elements are all at or below the light pollution level. Therefore, the HM concentrations corresponding to $I_{geo} = 0$ were taken as the disjunctive kriging thresholds.

Areas with pollution risk probability values above 0.5 are usually defined as high-risk hotspots and the distribution of pollution probabilities for the seven HMs is shown below (Fig. 5). the pollution risk probabilities for Cr, Zn, and Pb do not exceed 0.5 and there are no significant high-risk areas for these three HMs within the Tibetan Plateau.

The high-risk hotspots for Ni and As are mainly concentrated in the northwestern, central and eastern parts of the Tibetan Plateau, with a patchy distribution. 8% of the total area of the Tibetan Plateau is covered by areas with a probability of contamination above 0.5 for Ni and 12% of the total area of the Tibetan Plateau is covered by areas with a probability of contamination above 0.5 for As. The Qinghai-Tibet Plateau is located in the collision zone of the Eurasian plates,

Table 5 Soil accumulation index of heavy metals in the Qinghai-Tibet Plateau

Elements	Grassland	Woodland	Arable land	Waters	Urban, rural, and industrial and mining land	Unused land
Cr	−1.37	−0.99	−1.14	−0.90	−1.16	−1.03
Ni	−0.93	−0.86	−0.82	−0.70	−0.77	−0.79
Cu	−0.71	−0.61	−0.56	−0.68	−0.64	−0.65
Zn	−0.51	−0.34	−0.51	−0.69	−0.11	−0.78
As	0.59	−1.08	−0.98	−0.01	−0.48	−0.86
Cd	0.08	0.55	−0.01	0.28	0.91	−0.07
Pb	−1.45	−0.74	−1.74	−1.13	−0.55	−0.98

and the abundant thermal spring activities and relatively As-enriched soils and rocks are highly likely sources of As. In Tibet alone, there are nearly 700 hydrothermal activity areas with particularly high As concentrations, and the distribution of As under different land-use types also indicates that the

highest As concentration is found in water areas (Fig. 3). The Bangong Lake-Nujiang suture zone in the northwest is an important suture zone in the northern Qinghai-Tibet Plateau, where a large number of Ni-rich sulfide ultramafic rocks exist. The central region, located in the East Kunlun region
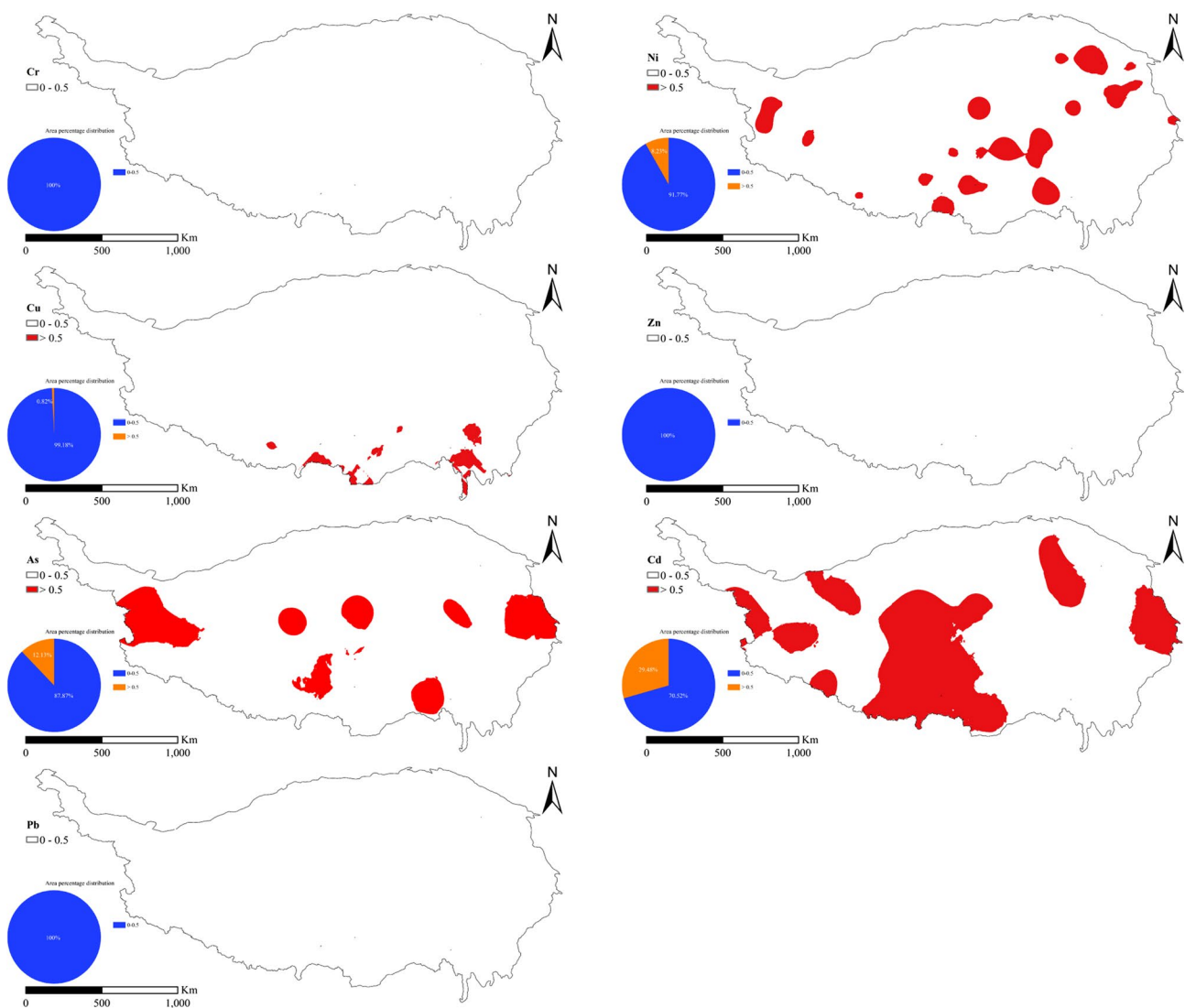
Fig. 5 Probability distribution of pollution risk of heavy metals in soils on the Qinghai-Tibet Plateau

of Qinghai Province, is rich in mineral resources, and a large number of Ni ores have been found throughout the region, and crustal extrusion and frequent geothermal activity have led to the northwest and central regions of the Tibetan Plateau being identified as Ni- and As-enriched hotspots.

Cu has the smallest area of high-risk hotspots, mainly in the cities of Shigatse, Shannan, and Linzhi, where dense population and heavy transport accelerate the enrichment of Cu in the soil.

The areas with a pollution risk probability of more than 0.5 for Cd account for 29% of the total area of the Tibetan Plateau and are mainly concentrated in the central, western, and eastern parts of the plateau. In recent years, industrial expansion has continued on the Tibetan plateau, investing in large-scale energy development and consumption, and cadmium, a major pollutant from industrial activities, can have an impact on the fragile ecological environment in and around the region. It is unlikely that all of the Cd in the soil comes from the plateau because on the plateau itself, there is little industry or agriculture, each of which is small in scale, and there are no obvious environmental pollution problems yet. It is possible that the Cd in the soil comes from the periphery of the plateau, which should be examined in terms of atmospheric deposition, the input of which has become a key process in the accumulation of Cd on the Qinghai-Tibet Plateau (Dong et al. 2015; Zhang et al. 2019; Xiao et al. 2000; Kerr 1979). This view has been supported by numerous studies, and the high elemental Cd content found in the sediments of Ximen Co lake on the Tibetan Plateau is due to the fact that anthropogenic pollutants in atmospheric aerosols from the west and South Asia can be carried to the Tibetan Plateau under the influence of the southwest monsoon (Yuan et al. 2014). Historical changes in Hg over the past 500 years were reconstructed from ice cores-lake cores on the Tibetan Plateau, indicating that anthropogenic emissions of pollutants from South Asia are the main cause of the rapid increase in atmospheric Hg deposition fluxes on the Tibetan Plateau (Kang et al. 2016). The results of atmospheric backward trajectories show that Gurenhekou Glacier and Yulong Xueshan are mainly influenced by inputs from the southwest and southeast air masses, with Gurenhekou Glacier being a possible potential source of trace elements due to its anthropogenic inputs from South Asia, in addition to possible influence from local industrial activities, resulting in higher levels and enrichment of Cd elements (Li et al. 2021). On the periphery of the Qinghai-Tibet Plateau, countries such as Iran and Kuwait from West Asia are important producers of oil, while India and Pakistan in South Asia have experienced rapid economic growth in recent decades, and the energy production and consumption required for the rapid development of these emerging economies is likely to lead to an upward trend in environmental pollution. In these processes, polluting the environment by emitting contaminated gases, metals, and organic compounds into the atmosphere results in pollutant transportation by westerly air currents and South Asian monsoon air currents, both of which reach the Qinghai-Tibet Plateau.

4 Conclusion

In this study, a methodology including semivariance function, the PMF source analysis model, and disjunctive kriging was integrated to determine the quantitative sources and risk areas of HMs in the soils of the Qinghai-Tibet Plateau based on the summary of previous research results. The mean concentrations of Cr, Ni, Cu, Zn, and Pb in the soils of the Qinghai-Tibet Plateau were mostly at low levels, although there were significant differences in the concentrations of seven HMs in soils of areas with different land-use types. Spatial autocorrelation was found for all seven heavy metals in the soils. Furthermore, through PMF model analysis and correlation analysis, four possible sources were identified. The risk probability of specific soil contaminations was evaluated using the disjunctive kriging method, which showed that Cr had no potential contamination, Ni, Cu, Zn, As, and Pb had potential contamination in localized areas, and Cd exhibited more extensive contamination. This indicates that Cd is the main pollutant in the soil in this region and that its reduction should be made an integral part of strategies, policies, and action plans of soil pollution management programs on the Tibetan Plateau.

Overall, this study provides useful information for identifying possible sources and areas of soil HM contamination on the Qinghai-Tibet Plateau, which will be useful for formulating targeted policies and measures for its reduction by HMs of the soil environment of the Qinghai-Tibet Plateau. This research can also give a contribution to promoting soil remediation and providing effective management recommendations for decision-makers.

Author contribution Haolin Du: conceptualization, methodology, software, investigation, formal analysis, writing—original draft; Jinsong Wang: conceptualization, funding acquisition, resources, supervision, writing—review and editing; Ying Wang: Visualization, investigation; Yubi Yao: resources, supervision; Xiaoyun Liu: software, validation; Yue Zhou: visualization, writing—review and editing.

Data availability The datasets used or analysed during the current study are available from the corresponding author upon reasonable request.

Declarations

Ethical approval Not applicable.

Consent to participate Not applicable.

Consent to publish Not applicable.

Competing interests The authors have no relevant financial or non-financial interests to disclose.

References

Bowen HJM (1979) Environmental chemistry of the elements. Academic Press, New York

Burgos P, Madejon E, Perez-De-Mora A, Cabrera F (2006) Spatial variability of the chemical characteristics of a trace-element-contaminated soil before and after remediation. Geoderma 130:157–175

Chandra R, Prusty BAK, Azeez PA (2014) Spatial variability and temporal changes in the trace metal content of soils: implications for mine restoration plan. Environ Monit Assess 186(6):3661–3671

Chen HY, Teng YG, Lu SJ, Wang YY, Wu J, Wang JS (2016) Source apportionment and health risk assessment of trace metals in surface soils of Beijing metropolitan. China Chemosphere 144(2):1002–1011

Chen NC, Zheng YJ, He XF, Li XF, Zhang XX (2017) Analysis of the report on the national general survey of soil contamination. J Agro-Environ Sci 36(9):1689–1692

Cheng SP (2003) Heavy metal pollution in China: origin, pattern and control. Environ Sci Pollut Res 10(3):192–198

Cong Y, Dong QJ, Xiao KY (2013) Study on metallogenic model and ore exploration of porphyry deposits in Sanjiang metallogenic belt. J Geol 37(4):562–569

Dong ZW, Kang SC, Qin X, Li XF, Qin DH, Ren JW (2015) New insights into trace elements deposition in the snow packs at remote alpine glaciers in the northern Tibetan Plateau, China. Sci Total Environ 529:101–113

Gao L, Xiao KY, Cong Y, Ding JH, Liu YL, Xiu QY, Wang SW, Hu GY (2016) Metallogenic characteristics and mineral resource potential of the southwestern Sanjiang Zn-Pb-Cu-Ag-Sb-Au metallogenic belt. Acta Geol Sin-Engl 90(7):650–667

Goovaerts P, Webster R, Dubois JP (1997) Assessing the risk of soil contamination in the Swiss Jura using indicator geostatistics. Environ Ecol Stat 4(1):31–48

Guan QY, Wang FF, Xu CQ, Pan NH, Lin JK, Zhao R, Yang YY, Luo HP (2018) Source apportionment of heavy metals in agricultural soil based on PMF: a case study in Hexi Corridor, northwest China. Chemosphere 193:189–197

Guan ZH, Li XG, Wang L (2017) Heavy metal enrichment in roadside soils in the eastern Tibetan Plateau. Environ Sci Pollut Res 25(8):7625–7634

Guo BX, Liu YQ, Zhang F, Hou JZ, Zhang HB, Li CL (2018) Heavy metals in the surface sediments of lakes on the Tibetan Plateau, China. Environ Sci Pollut Res 25:3695–3707

Hou D, O'Connor D, Nathanail P, Tian L, Ma Y (2017) Integrated GIS and multivariate statistical analysis for regional scale assessment of heavy metal soil contamination: a critical review. Environ Pollut 231:1188–1200

Hu BF, Zhao RY, Chen SC, Zhou Y, Jin B, Li Y, Shi Z (2018) Heavy metal pollution delineation based on uncertainty in a coastal industrial city in the Yangtze river delta, China. Int J Env Res Pub He 15(4):710–722

Huang JH, Guo ST, Zeng GM, Li F, Gu YL, Shi YH, Shi LX, Liu WC, Peng SY (2018) A new exploration of health risk assessment quantification from sources of soil heavy metals under different land use. Environ Pollut 243:49–58

Huang X, Sillanpää M, Duo B, Gjessing ET (2008) Water quality in the Tibetan Plateau: metal contents of four selected rivers. Environ Pollut 156:270–277

Jin YL, David O, Ok YS, Tsang DWC, Liu A, Hou DY (2019) Assessment of sources of heavy metals in soil and dust at children's playgrounds in Beijing using GIS and multivariate statistical analysis. Environ Int 124:320–328

Juang KW, Lee DY (2000) Comparison of three non-parametric Kriging methods for delineating heavy-metal contaminated soils. J Environ Qual 29(1):197–205

Kang S, Huang J, Wang F, Zhang Q, Zhang Y, Li C, Wang L, Chen P, Sharma CM, Li Q, Sillanpää M, Hou J, Xu B, Guo J (2016) Atmospheric mercury depositional chronology reconstructed from lake sediments and ice core in the Himalayas and Tibetan Plateau. Environ Sci Technol 50:2859–2869

Kerr RA (1979) Global pollution:is the arctic haze actually industrial smog? Science 205:290–293

Lark RM, Ferguson RB (2004) Mapping risk of soil nutrient deficiency or excess by disjunctive and indicator kriging. Geoderma 118:39–53

Lee PK, Kang MJ, Yu S, Kwon YK (2020) Assessment of trace metal pollution in roof dusts and soils near a large Zn smelter. Sci Total Environ 713:136536

Li DW (2010) Temporal-spatial structure of intraplate uplift in the Qinghai-Tibet Plateau. Acta Geol Sin-Engl 84(1):105–134

Li RC, Shen BS, Wu XB, Yang FS, Guo ZM (2021) Spatial distribution and source analysis of trace elements in typical mountain glaciers on the Qinghai-Tibet Plateau. J Glaciol Geocryol 43(5):1277–1289 (in chinese)

Li SH, Wang MG, Yang Q, Wang H, Zhu JM, Zheng BS, Zheng Y (2013) Enrichment of arsenic in surface water, stream sediments and soils in Tibet. J Geochem Explor 135(1):104–116

Lin Z, Chao L, Wu CZ, Hong W, Hong T, Hu XS (2018) Spatial analysis of carbon storage density of mid-subtropical forests using geostatistics: a case study in Jiangle county. Southeast China Acta Geo 37(1):90–101

Liu A, Ma YK, Gunawardena JMA, Egodawatta P, Ayoko GA, Goonetilleke A (2018) Heavy metals transport pathways: the importance of atmospheric pollution contributing to stormwater pollution. Ecotox Environ Safe 164:696–703

Ministry of Ecology and Environment of the People's Republic of China (MEP) (2018) Soil environmental quality–risk control standards for soil contamination of agricultural land. Chinese National Standard Agency, Beijing (in Chinese)

Müller G (1969) Index of geoaccumulation in sediments of the Rhine River. Geol J 2(3):108–118

Paatero P (1997) Least squares formulation of robust non-negative factor analysis. Chemometr Intell Lab 37(1):23–35

Reff A, Eberly SI, Bhave PV (2007) Receptor modeling of ambient particulate matter data using positive matrix factorization: review of existing methods. J Air Waste Manage 57(2):146–154

Romic M, Romic D (2003) Heavy metals distribution in agricultural topsoils in urban area. Environ Geol 43:795–805

Sheng JJ, Wang XP, Gong P, Tian LD, Yao TD (2012) Heavy metals of the Tibetan top soils: level, source, spatial distribution, temporal variation and risk assessment. Environ Sci Pollut Res 19(8):3362–3370

Song YC, Hou ZQ, Yang TN, Zhang HR, Yang ZS, Tian SH, Liu YC, Wang XH, Liu YX, Xue CD, Wang GH, Li Z (2011) Sediment-hosted Himalayan base metal deposits in Sanjiang region: characteristics and genetic types. Acta Petrol Mineral 30(3):355–380 (in Chinese)

Steiger B, Webster R, Schulin R, Lehmann R (1996) Mapping heavy metals in polluted soil by disjunctive kriging. Environ Pollut 94:205–215

Tian SH, Liang T, Li KX, Wang LQ (2018) Source and path identification of metals pollution in a mining area by PMF and rare earth element patterns in road dust. Sci Total Environ 633:958–966

Wei FS, Chen JS, Wu YY, Zheng CJ (1991) Study on the background values of soil environment in China. Environ Sci 12(4):12–19 (in Chinese)

Wu CF, Huang JY, Minasny B, Zhu H (2017) Two-dimensional empirical mode de-composition of heavy metal spatial variation in agricultural soils. Southeast China Environ Sci Pollut Res 24(9):8302–8314

Wu DT, Zhang DW (1992) Study on the variation of nickel background value in topsoil of china. Environ Monit China 3:49–53 (in Chinese)

Wu J, Duan D, Lu J, Luo Y, Wen X, Guo X, Boman BJ (2016) Inorganic pollution around the Qinghai-Tibet Plateau: an overview of the current observations. Sci Total Environ 550:628–636

Wu J, Lu J, Li LM, Min XY, Luo YM (2018) Pollution, ecological-health risks, and sources of heavy metals in soil of the northeastern Qinghai-Tibet Plateau. Chemosphere 201:234–242

Xiao CD, Qin DH, Yao TD, Ren JW, Li YF (2000) Global pollution shown by lead and cadmium contents in precipitation of polar regions and Qinghai-Tibetan Plateau. Chin Sci Bull 9:847–853

Yang RQ, Yao TD, Xu BQ, Jiang GB, Xin XD (2007) Accumulation features of organochlorine pesticides and heavy metals in fish from high mountain lakes and Lhasa River in the Tibetan Plateau. Environ Int 33:151–156

Yoon SJ, Hong S, Lee C, Lee J, Kim T, Lee J, Kim B, Noh J, Kwon BO, Khim JS (2022) 10 years long-term assessment on characterizing spatiotemporal trend and source apportionment of metal(loid)s in terrestrial soils along the west coast of South Korea. Sci Total Environ 826:154214

Yuan HZ, Liu EF, Shen J, Zhou HJ, Geng QF, An SQ (2014) Characteristics and origins of heavy metals in sediments from Ximen Co Lake during summer monsoon season, a deep lake on the eastern Tibetan Plateau. J Geochem Explor 136:76–83

Zhang XW, Wei S, Sun QQ, Wadood SA, Guo BL (2018) Source identification and spatial distribution of arsenic and heavy metals in agricultural soil around Hunan industrial estate by positive matrix factorization model, principle components analysis and geo statistical analysis. Ecotox Environ Safe 159:354–362

Zhang YF, Li SH, Zheng LR, Chen JG, Zheng Y (2016) Evaluation of arsenic sorption and mobility in stream sediment and hot spring deposit in three drainages of the Tibetan Plateau. Appl Geochem 77:89–101

Zhang ZS, Zheng DM, Xue ZS, Wu HT, Jiang M (2019) Identification of anthropogenic contributions to heavy metals in wetland soils of the Karuola Glacier in the Qinghai-Tibetan Plateau. Ecol Indic 98:678–685

Zhao JA (2002) Development prospect of communication and transportation networks of the Qinghai-Tibet Plateau in the earlier stage of 21st century. Resour Sci 4:5–10